

of Kattan and Adler. Hence, from Equation (3) it should be possible to calculate  $D/l_m^2$  if  $\beta$  were known.

The value of  $\beta$ , and hence  $D/l_m^2$ , at any axial position can be found by multiplying the slope of the plot of  $\eta$  versus  $Z$  as shown in Figure 1 (reproduced from the paper by Kattan and Adler) by the velocity of the fluid in the reactor.  $\eta$  is defined as the total number of coalescences experienced by the fluid elements between the entrance and any axial position  $Z$  divided by the total number of fluid elements. For example, the slope of the curve is 0 up to a distance of about 0.15 in. from the inlet, then it rises very sharply and reaches a constant value. If one calculates  $D/l_m^2$  from this constant value of slope,  $D/l_m^2$  turns out to be 3.25 (velocity of fluid in the reactor is taken as 16 in./sec.). However, if one assumes a straight line relationship from the origin to the ordinate, at  $Z = 2.0$  in., the value of  $D/l_m^2$  turns out to be 4.53 which is exactly the same value used for  $D/\delta^2$  in the single-slab diffusion model of Mao and Toor. This suggests the equivalence between the slab-diffusion model and the coalescence dispersion model for a very rapid second order reaction with unmixed feed or a tracer mixing process in a tubular reactor.

As can be seen in the differential equation model of Mao and Toor and in the coalescence-dispersion models, the reaction terms do not interact with diffusion terms and hence the equivalence ought to remain valid for any value of the reaction rate constant. That is, the mixing as depicted in the model is unaffected by the chemical reaction. Of course both types of models do represent the experimental data of Vassilatos and Toor for all reaction rates.

## ACKNOWLEDGMENT

The authors are grateful for a National Science Foundation grant (GK-10043) which supported this work.

## NOTATION

$\bar{c}^2$	= mean square concentration fluctuation
$D$	= molecular diffusion coefficient
$l_m$	= scalar microscale of turbulence
$N$	= number of drops in the reactor
$t$	= time
$Z$	= axial position (inches)

## Greek Letters

$\beta$	= coalescence rate per unit fluid element
$\delta$	= slab thickness
$\sigma^2$	= variance of tracer concentration distribution
$\eta$	= mixing characteristic, dimensionless

## LITERATURE CITED

1. Evangelista, J. J., S. Katz, and R. Shinnar, *AIChE J.*, **15**, 843 (1969).
2. Harris, I. J., and R. D. Srivastava, *Can. J. Chem. Eng.*, **46**, 66 (1968).
3. Kattan, A., and R. J. Adler, *AIChE J.*, **13**, 580 (1967).
4. Mao, K. W., and H. L. Toor, *AIChE J.*, **16**, 49 (1970).
5. Rao, D. P., and I. J. Dunn, *Chem. Eng. Sci.*, **25**, 1275 (1970).
6. Spielman, L. A., and O. Levenspiel, *Chem. Eng. Sci.*, **20**, 247 (1965).
7. Vassilatos, G., and H. L. Toor, *AIChE J.*, **11**, 666 (1965).

# An Experimental Investigation of a Porous Medium Model with Nonuniform Pores

R. J. PAKULA and R. A. GREENKORN

School of Chemical Engineering  
Purdue University, Lafayette, Indiana 47907

Many techniques have been employed to describe mathematically the flow of fluids in porous media (1). In the majority of cases only one particular phenomenon was investigated. An expression for the particular property is usually derived empirically and contains a term characteristic of the medium. These tortuosity and heterogeneity factors have been derived for a number of types of porous media (2).

To study the microstructure of porous media and its effect on the observable bulk properties more systematically, several statistical models have been postulated. One of the first models was that of a bundle of straight capillary tubes; another depicted the medium as a series of mixing cells. Both have been used successfully to a degree, even though they are simple models. Although the void spaces

in most cases can be visualized as capillaries, their arrangement is highly disordered, and the sizes of the voids are definitely nonuniform. Fatt (3) has constructed network models which include nonuniformity to predict permeability and capillary pressure. De Josselin De Jong (4) and Saffman (5) postulated random network models with uniform properties to predict the dispersion in such models. Haring and Greenkorn (6) postulated a statistical model which includes nonuniformity by allowing pore radii and pore lengths to be distributed. They have calculated the properties of such a model by fitting the radii and lengths with two parameter distribution functions. These parameters are related to the first and second moments of the microstructure of the medium. Equations for the various flow properties of the medium have been derived by integrating over joint distributions of the models.

This presents an experimental investigation of the measurement of certain properties of a porous medium to

R. J. Pakula is with Parke Davis and Company, Detroit, Michigan 48230.

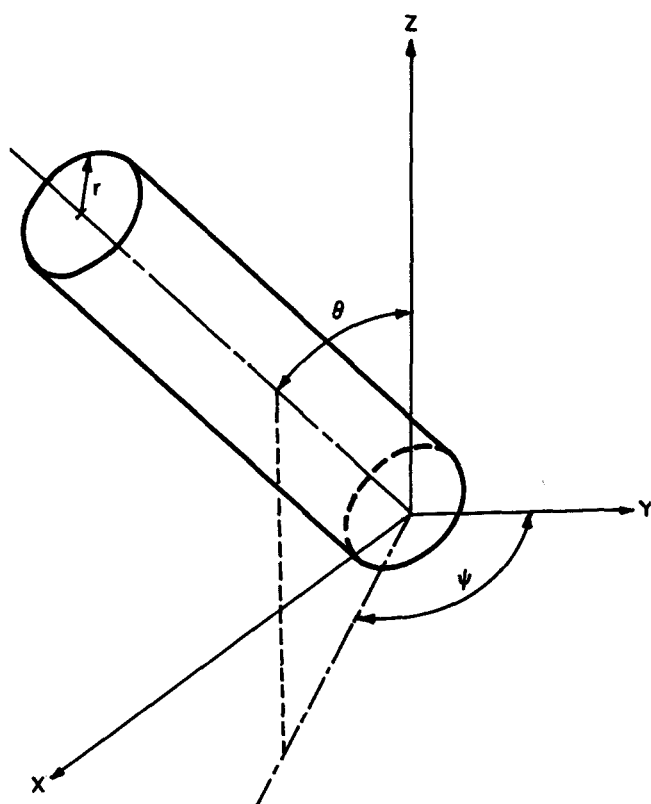


Fig. 1. Description of elemental pore.

determine the distribution parameters in the model of Haring and Greenkorn (6) and to predict the macroscopic properties using these parameters. These experiments are meant to demonstrate that the results of the statistical models are realistic and therefore can be used to draw certain general conclusions about the characteristics of porous media. In addition, the data are a unique set of measurements of the macroscopic properties of a nonuniform unconsolidated porous medium that is very well described.

## DESCRIPTION OF THE STATISTICAL MODEL

The reader is referred to Haring and Greenkorn (6) for a detailed derivation of the model. In this model an elemental pore is assumed, as shown in Figure 1. The length, radius, and orientation angles  $\theta$  and  $\psi$  are assumed independent. The dimensionless length

$$l^* = \frac{l}{L}; \quad 0 \leq l \leq L \quad \text{and} \quad 0 \leq l^* \leq 1 \quad (1)$$

where  $L$  is the longest pore, and the dimensionless radius,

$$r^* = \frac{r}{R}; \quad 0 \leq r \leq R \quad \text{and} \quad 0 \leq r^* \leq 1 \quad (2)$$

where  $R$  is the largest radius pore, are distributed according to the beta function. The values for the incomplete beta function

$$B(x; p_1, p_2) = \int_0^x \frac{(p_1 + p_2 + 1)!}{p_1! p_2!} x^{p_1} (1-x)^{p_2} dx \quad (3)$$

are tabulated (7) so a curve of  $P_c^*$  versus  $S$  can be constructed by using the tabulated values for

$$(1-S) = B\left(\frac{1}{P_c^*}; \alpha + 2, \beta\right) \quad (4)$$

The permeability of the model is found by relating the average velocity in a pore to the average velocity in the network.

$$\frac{k}{\phi} = \frac{\langle r \rangle^2}{24} \frac{(\alpha + 2)(\alpha + \beta + 2)}{(\alpha + \beta + 3)(\alpha + 1)} \quad (5)$$

In terms of the parameters of the length and radius distribution the expression for longitudinal dispersion is

$$K_L = \frac{1}{12} \frac{(a+2)(a+b+2)}{(a+1)(a+b+3)J^2} \langle l \rangle$$

$$V \ln \left[ \frac{27}{2} \frac{(a+b+3)^2}{(a+1)J^3} \frac{VT}{\langle l \rangle} \right] \quad (6)$$

and the expression for the transverse dispersion is

$$K_T = \frac{3}{16} \frac{(a+2)(a+b+2)}{(a+1)(a+b+3)J} \langle l \rangle V \quad (7)$$

where

$$J = \frac{(\alpha+1)(\alpha+2)(\alpha+\beta+4)(\alpha+\beta+5)}{(\alpha+3)(\alpha+4)(\alpha+\beta+2)(\alpha+\beta+3)} \quad (8)$$

## EXPERIMENTAL PROCEDURES

All the experiments were in an unconsolidated porous medium consisting of glass beads with a specified range of bead diameters of 840-590  $\mu$  and specified density of 2.40 to 2.50 g./cu.cm. (see Table 1). The beads were contained in cylindrical plexiglas columns 6 in. long, with an inside diameter of 1 1/8 in. The columns were packed by slowly pouring the beads in while the column was vibrated on a mechanical vibrating unit. The beads were held rigidly in place after packing by a plexiglass cap and a plug was screwed onto the ends. Rubber O-rings provided a tight seal.

### Porosity

Before packing the beads, the internal volume of the cylinder was computed. After the column was packed, the dry weight was recorded and then the column was saturated with water. From the dry and saturated weights the void volume and void fraction were obtained. The porosity for each model

TABLE 1. SUMMARY OF BEAD PACK PROPERTIES

Particle Size Range	840-590 micron	(Specified)
Average pore radius	85 micron	(Calculated)
Largest pore radius	329 micron	(Calculated)
Average pore length	358 micron	(Estimated)
Largest pore length	375 micron	(Calculated)
Porosity	0.354	(Measured)
Permeability	175 darcies	(Calculated)
	158 darcies	

### Experimental Values of Porosity

Based on Water Uptake	Based on Average Bead Density
0.361	0.326
0.358	0.335
0.355	0.311
0.350	0.327
0.358	0.334
0.350	0.341
0.347	0.328

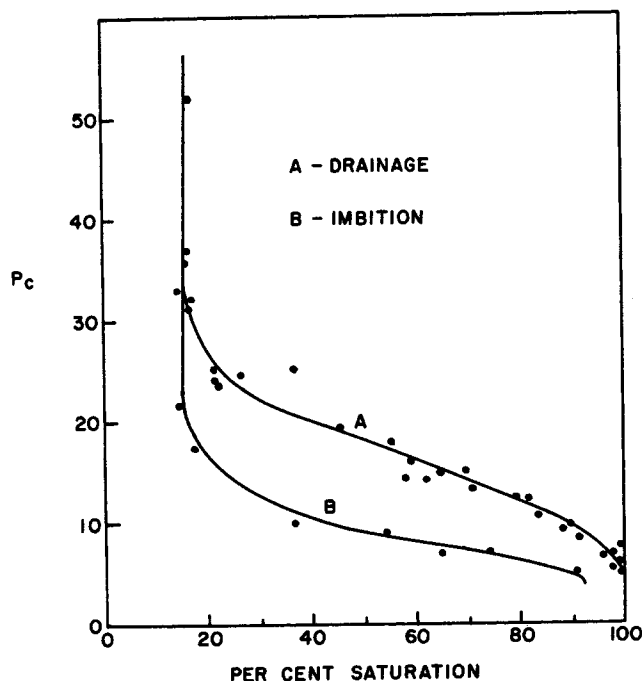


Fig. 2. Experimental capillary pressure curve.

was determined by the liquid saturation method and also by the average bead density.

#### Capillary Pressure

To determine the relationship between capillary pressure and water saturation, a special cap was constructed for the models. A spacing was provided in this cap to hold a  $\frac{1}{4}$  in. thick by  $1\frac{1}{8}$  in. diameter porous ceramic plate. This commercially available ceramic plate is water wet and will allow the passage of water but not gas up to a pressure of 2 atm. After this plate was saturated and inserted in the column, the beads were packed by the same procedure as outlined previously.

The technique employed for obtaining the capillary pressure versus saturation curves is reported in the literature (8, 9). The results obtained are in good agreement with published data on small packs of glass beads of similar diameter (10, 11). Figure 2 shows the experimentally obtained capillary pressure versus saturation curve for inhibition and drainage.

#### Permeability

The permeabilities of the model were determined from Darcy's Law written in the form

$$k = \frac{L}{\rho g A} \frac{Q}{\Delta h} \quad (9)$$

by timing the rate of flow under a given pressure drop of fluid through the model.

#### Dispersion

To obtain the values of the length parameters, a measure of the transverse and longitudinal dispersion at one velocity, together with an estimate of the average pore length, is needed. Equations (10) and (11)

$$K_L = \frac{(\bar{Z} - \bar{V}T)^2}{2T} \quad (10)$$

$$K_T = \frac{\bar{X}^2}{2T} = \frac{\bar{Y}^2}{2T} \quad (11)$$

define the necessary dispersion coefficients, provided the terms  $Z$ ,  $X$ ,  $\bar{V}$ , and  $T$  for a marked particle can be determined. The

distance  $Z$  and  $X$  can be fixed by the location of measuring electrodes in a given medium.

The particular method used to obtain the concentration changes with time was to use silver-silver chloride electrodes to measure changes of chloride ion concentration (12, 13). The model is initially saturated with .02 M KCl. This resident fluid is displaced with a 0.4 M solution of KCl at a constant flow rate provided by a positive displacement pump. The concentration at a point is measured as the potential difference between a silver-silver chloride electrode at that point and a saturated calomel reference electrode. The potential difference between these two electrodes is a function of the chloride ion concentration and thus provides the necessary information.

The electrodes were inserted into the model by drilling holes in the cap and sealing with epoxy. For the measurement of transverse dispersion 12 probes were used. There were 6 probes  $\frac{1}{2}$  in. from the inlet and 6 probes  $1\frac{1}{2}$  in. from the inlet. At each distance into the pack, there were 3 probes at a radius of  $11/32$  in. and 3 at a radius of  $15/32$  in. After the probes were inserted the beads were packed in the usual manner. This arrangement of probes made it possible to determine the time required for a marked particle (concentration) to travel from a point ( $Z_1, R_1$ ) to another point ( $Z_2, R_2$ ) where the length  $Z_2$  is greater than  $Z_1$  and the radius  $R_2$  greater than  $R_1$ .

Longitudinal dispersion was determined from concentration measurements between electrodes  $\frac{1}{4}$  in. in at the center of each end of the model. Dispersion measurements were made at three flow rates with duplicates at each flow rate.

#### RESULTS

The summary of the bead pack properties is given in Table 1. The permeability for these packs is 175 Darcys. The capillary pressure data was used to obtain the parameters of the radius distribution and  $P_c(R)$  was determined from capillary pressure curves. The reduced capillary pressure curve shown in Figure 3 was fit with the best fit of the incomplete beta function. The tabulated values which provided the best fit correspond to  $\alpha = 0$  and  $\beta = 2$ . With this information it was possible to solve for the average pore radius. For this medium, average pore radius was 0.00855 cm. or 85.5  $\mu$ .

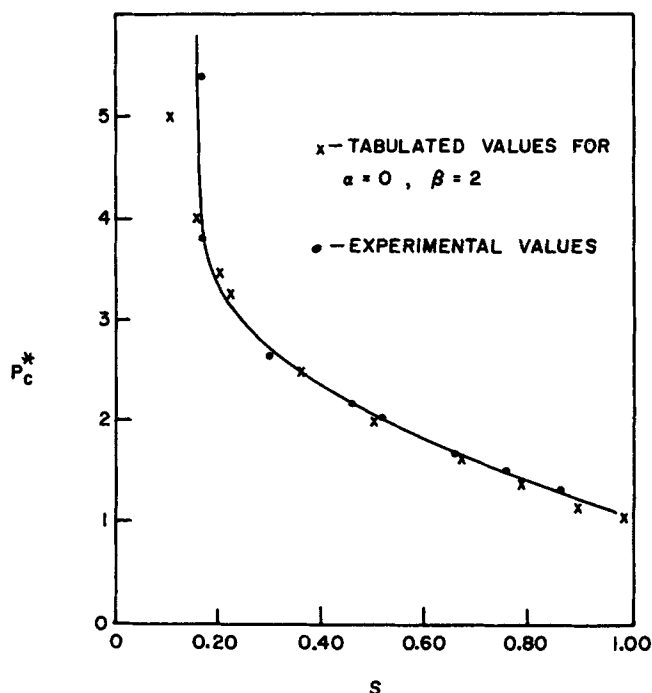


Fig. 3. Reduced capillary pressure versus  $s$ .

TABLE 2. EXPERIMENTAL AND CALCULATED  
DISPERSION COEFFICIENTS

Velocity, cm./sec.	$K_L$ , sq.cm./sec. $\times 10^3$		$K_T$ , sq.cm./sec. $\times 10^4$	
	Meas.	Calc.	Meas.	Calc.
0.0273	8.62	(8.62) <sup>*</sup>	6.08	(6.08) <sup>*</sup>
0.0156	6.02	5.55	3.53	3.48
0.0078	1.84	2.78	2.05	1.74

\* These values are the same because the model parameters  $a$  and  $b$  were determined at this velocity.

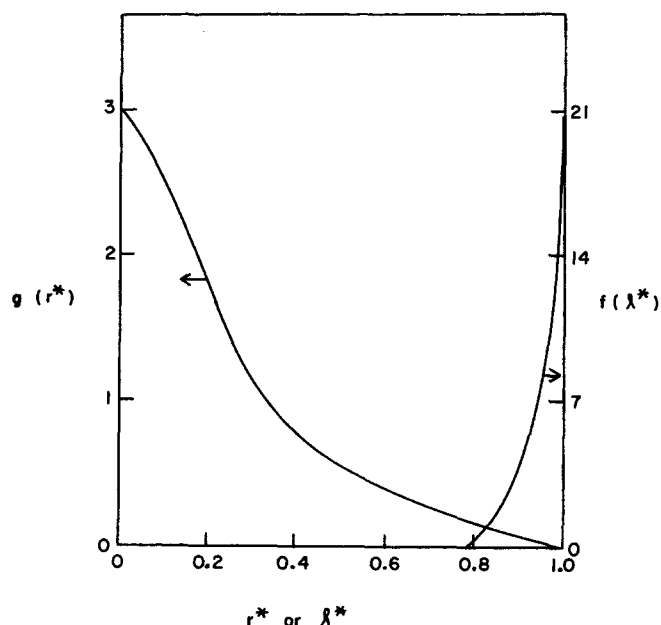


Fig. 4. Radius and length distributions.

The average pore radius can be determined without the knowledge of permeability. All that is required is  $\alpha$ ,  $\beta$  and the value of  $P_c(R)$ , all of which are found from the capillary pressure versus saturation data. From  $P_c(R)$  the value of  $R$  the largest pore radius can be found. This value of  $R$  (329  $\mu$ ) may be used to find the average pore radius. When the value of  $R$  together with  $\alpha$ ,  $\beta$  and the porosity are known the value of permeability is obtained. The calculated permeability is 158 Darcys, which is within 10% of the measured value of 175 Darcys.

Experimental values of  $K_T$  and  $K_L$  are shown in Table 2 along with the theoretical values. From these values:  $a = 20$ ,  $b = 0$  and the average pore length = 0.0358 cm. Knowledge of the length and radius distribution parameters not only gives us a quantitative relationship for permeability and dispersion, but also a concept of the length and radius distribution. Figure 4 shows the probability density function for the radius and length distribution functions. From these curves we see that both the radius and length distribution are skewed, with length distribution being almost uniform. Both results are in agreement with the data reported in the literature (1, 3, 14) and with those intuitively expected from this model.

## CONCLUSIONS

By means of experiment the parameters of the length and radius distributions of the statistical model of Haring and Greenkorn (6) have been evaluated. The resulting expressions predict permeability and dispersion coefficients

in reasonable agreement with the experimentally measured values. The results show the statistical model is capable of predicting macroscopic flow parameters as a result of independent parameter measurements and statistical models have definite meaning in characterization of a porous medium.

## NOTATION

$a, b$  = parameters in length distribution  
 $a_{ijkl}$  = dispersivity tensor  
 $c$  = concentration  
 $D_{ij}$  = dispersion tensor  
 $h$  = height  
 $k$  = permeability  
 $K_L$  = longitudinal dispersion  
 $K_T$  = transverse dispersion  
 $l$  = pore length  
 $L$  = length of longest pore  
 $p$  = pressure  
 $P_c$  = capillary pressure  
 $q$  = volumetric flow rate  
 $r$  = pore radius  
 $R$  = radius of largest pore  
 $S$  = saturation  
 $T$  = time  
 $v$  = velocity  
 $V$  = average pore velocity  
 $V$  = velocity along most probable path  
 $X, Y, Z$  = displacements in the  $x, y, z$  directions

## Greek Letters

$\alpha, \beta$  = parameters in radius distribution  
 $\phi$  = porosity  
 $\psi$  = angle from  $y$  axis projected in  $xy$  plane  
 $\rho$  = density  
 $\theta$  = angle from  $z$  axis  
 $\mu$  = viscosity

## Subscripts

$T$  = time  
 $Z$  = coordinate,  $z$  direction

## LITERATURE CITED

1. Scheidegger, A. E., "The Physics of Flow Through Porous Media," MacMillan, New York (1957).
2. Perkins, T. K., and O. C. Johnston, *Trans. AIME*, **228**, 70 (1963).
3. Fatt, I., *Trans. AIME*, **207**, 144 (1956).
4. De Josselin De Jong, G., *Trans. Amer. Geophys. Union*, **39**, 67 (1958).
5. Saffman, P. G., *J. Fluid Mech.*, **6**, 321 (1959).
6. Haring, R. E., and R. A. Greenkorn, *AIChE J.*, **16**, 477 (1970).
7. Pearson, K., Ed., "Tables of the Incomplete Beta-Function," The University Press, Cambridge (1934).
8. Purcell, W. R., *Trans. AIME*, **186**, 39 (1949).
9. Calhoun, J. C., "Fundamentals of Reservoir Engineering," Univ. Oklahoma Press, Norman, Oklahoma (1953).
10. Harris, C. C., and N. R. Morrow, *Trans. AIME*, **23**, 15 (1965).
11. Henderson, J. H., J. Naas, and R. J. Wygal, *Trans. AIME*, **225**, 13 (1962).
12. Brown, W. O., *Trans. AIME*, **210**, 190 (1957).
13. Shoemaker, D. P., and C. W. Garland, "Experiments in Physical Chemistry," McGraw-Hill, New York (1962).
14. Richardson, J. G., in "Handbook of Fluid Mechanics," V. L. Streeter, Ed., p. 165 McGraw-Hill, New York (1961).